# CHIRP MODULATION

Chirp modulation, which has been extensively used in radar systems since World War II (1), was introduced by Germans at the end of the war in the design of a pulse radar called Kugelschale (2). The main reason behind the introduction of the chirp modulation to pulse radar technology was its anti-jamming properties. The technique was later rectified and enriched during 1940s, and since the early 1950s chirp modulation has been used in radar systems to solve the conflicting requirements of simultaneous long-range and high-resolution performance (3).

The first possible applications of chirp modulation in data communications were considered in the early 1960s. Winkler (4) proposed a system in which the linear frequency sweep of the chirp signal assumed a positive or negative slope corresponding to binary data symbols $+1$ and $-1$, respectively. Since then, chirp modulation and its several modifications and generalizations have been considered for both spread-spectrum and narrowband applications where immunity against Doppler frequency shift (5) and fading due to multipath propagation is important.

These were never intended to replace other bandpass digital modulation schemes, like (5) amplitude shift keying (ASK), phase shift keying (PSK) or frequency shift keying (FSK), but rather considered useful techniques for niche applications. These applications have included but have not been limited to aircraft-ground data links via satellite repeaters (6), low-rate data transmission in the high-frequency (HF) band (7), narrowband data transmission (8), indoor wireless local area networks (WLANs) (9), data communications utilizing a building's power cabling (10), and acoustic modems for underwater communications (11).

## CLASSIFICATION OF CHIRP AND RELATIVE MODULATIONS

Since publication of the first idea about possible use of chirp modulation (CM) in digital communication systems in the early 1960s, several authors have proposed different digital modulation schemes based on incorporating CM to achieve desired characteristics of the modulated signal. In this section, we classify some of these schemes into (1) pure CM, (2) generalized CM, and (3) hybrid CM techniques.

### Pure Chirp Modulation

CM or linear frequency modulation, in its pure form, refers to the creation of such a waveform in which the instantaneous frequency of the signal changes linearly between the lower and upper frequency limits. This is graphically illustrated in the Fig. 1, which shows the two basic types of chirp pulses and their instantaneous frequency profiles.

For the positive chirp $c_p(t)$, the instantaneous frequency $f_i^+(t)$ increases during the pulse duration and is expressed as

$$f_i^+(t) = f_l + (f_u - f_l)\frac{t}{T}, \quad 0 \le t \le T$$

where $f_l$ and $f_u$ are the lower and the upper frequency limits, respectively, and $T$ is the duration of the chirp pulse. In the case of the negative chirp $c_n(t), f_i^-(t)$ decreases during the pulse duration and is given by

$$f_i^-(t) = f_u - (f_u - f_l)\frac{t}{T}, \quad 0 \le t \le T$$

Introducing modulation index $h$, defined in the same way as for binary frequency shift keying (FSK) (5)

$$h = (f_u - f_l)T = \Delta f T$$

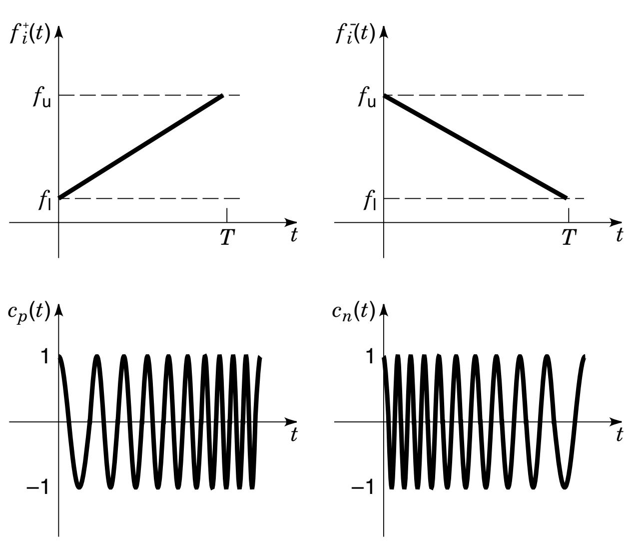


**Figure 1.** Illustration of positive and negative chirp pulses and their instantaneous frequency profiles.

we can express $f_i^+(t)$ as

$$f_i^+(t) = \left(f_c - 0.5\frac{h}{T}\right) + \frac{ht}{T^2}, \quad 0 \le t \le T$$

where $f_c$ denotes the central frequency of the chirp pulse, sometimes referred to as the carrier frequency. Similarly, $f_i^-(t)$ is given by

$$f_i^-(t) = \left(f_c + 0.5\frac{h}{T}\right) - \frac{ht}{T^2}, \quad 0 \le t \le T$$

Since CM is equivalent to linear FM within each pulse, we can describe the waveform $c_p(t)$, for $0 < t \le T$, as

$$\begin{aligned} c_p(t) &= A\cos\left[2\pi\int_0^t f_i^+(\tau)\,d\tau + \phi_0\right] \\ &= A\cos\left[2\pi\int_0^t \left(f_c - 0.5\frac{h}{T} + \frac{h\tau^2}{T^2}\right)d\tau + \phi_0\right] \end{aligned} \tag{1}$$

where $A$ is the signal amplitude, usually being a constant of time, and $\phi_0$ denotes an initial value of the phase. Performing the integration in Eq. (1) yields

$$c_p(t) = A\cos\left[2\pi\left(f_c - 0.5\frac{h}{T}\right)t + \frac{\pi h t^2}{T^2} + \phi_0\right];\ 0 < t \le T \tag{2}$$

By analogy, we can write

$$c_n(t) = A\cos\left[2\pi\left(f_c + 0.5\frac{h}{T}\right)t - \frac{\pi h t^2}{T^2} + \phi_0\right];\ 0 < t \le T \tag{3}$$

Assuming, as Winkler in Ref. 4, that $c_p(t)$ is used to transmit binary 1 and $c_n(t)$ to transmit $-1$, we can regard a sequence of pulses $c_p(t)$ and $c_n(t)$ bearing the binary data sequence $\boldsymbol{I} = \{I_1, I_2, \ldots, I_k, \ldots I_n\}$, $I_k \epsilon \{-1, 1\}$, as a general form for a pure CM signal $c(t, \boldsymbol{I})$,

$$c(t, \boldsymbol{I}) = A\sum_{k=1}^{\infty}\xi(t - kT, I_k) \tag{4}$$

where

$$\xi(t, I_k) = \begin{cases}\cos\left[2\pi\left(f_c - \dfrac{I_k h}{2T}\right)t + \dfrac{\pi I_k h t^2}{T^2} + \phi_k\right], & 0 < t \le T \\ 0, & \text{otherwise}\end{cases} \tag{5}$$

$I_k \in \{-1, 1\}$, and $\phi_k$ is the starting phase of a $k$th modulated signal pulse. Usually, there are no restrictions placed on the distribution of $\phi_k$ in the pure CM scheme.

To calculate useful characteristics of the modulated signal, it is convenient to represent it as a bandpass signal (5). In such a notation, we represent the CM signal given by Eqs. (4) and (5) as

$$c(t, \boldsymbol{I}) = A\,\mathrm{Re}\left[\sum_{k=0}^{\infty} v(t - kT, I_k)\right] \tag{6}$$

where

$$v(t, I_k) = \begin{cases}\exp[j2\pi h I_k q_p(t)]\exp[j(2\pi f_c t + \phi_k)], & 0 < t \le T \\ 0, & \text{otherwise}\end{cases} \tag{7}$$

$j = \sqrt{-1}$, and $q_{\mathrm{p}}(t)$ is an elementary phase pulse. Comparing Eqs. (5) and (7), it is easy to note that the CM characteristic elementary phase pulse $q_{\mathrm{p}}(t)$ is given by

$$q_{\mathrm{p}}(t) = \begin{cases} \dfrac{t^2}{2T^2} - \dfrac{t}{2T}, & 0 < t \leq T \\ 0, & \text{otherwise} \end{cases}$$

In general, the initial phase $\phi_{\mathrm{k}}$ of each CM pulse can be different and take any value from the interval $[0, 2\pi)$. For simplicity of representation, let us assume here that the considered CM signal is of a continuous phase modulation (CPM) (5) type. Because the phase increment $\Delta\phi$ introduced by the baseband component $b(t, I_{\mathrm{k}})$ of $v(t, I_{\mathrm{k}})$,

$$b(t, I_{\mathrm{k}}) = \begin{cases} \exp[j2\pi h I_{\mathrm{k}} q_{\mathrm{p}}(t)], & 0 < t \leq T \\ 1, & \text{otherwise} \end{cases}$$

is equal to zero for $t = T$ (i.e., at the end of each CM pulse), the assumption of the phase continuity in the CM signal has no influence on $b(t, I_k)$ and therefore no influence on important signal characteristics.

Hence, we can describe the CM signal as

$$c(t, \boldsymbol{I}) = A\,\mathrm{Re}\{\beta(t, \boldsymbol{I}) \exp[j(2\pi f_{\mathrm{c}} t + \phi_0)]\} \tag{8}$$

where $\phi_0$ is an initial phase of the carrier wave and $\beta(t, \boldsymbol{I})$ is the equivalent CM baseband signal

$$\beta(t, \boldsymbol{I}) = \sum_{k=-\infty}^{\infty} b(t - kT, I_{\mathrm{k}}) \tag{9}$$

Since the total phase increment $\Delta\phi$ introduced by $b(t, I_{\mathrm{k}})$ is equal to zero, there is a lack of correlation among the modulated signal pulses. This leads to rather poor error performance of the pure CM compared with other modulation schemes in the additive white gaussian noise (AWGN) channel (12). Thus pure CM is rarely considered for narrowband systems. In contrast, the excellent performance of wideband CM signals, $h \gg 1$, in mobile environments experiencing both multipath propagation and Doppler shift (7,9,11), or in the presence of continuous wave (CW) jammers (10) increased interest in applying CM or CM-like signals in spread spectrum (SS) (5) systems.

## Generalized Chirp Modulation

A method for overcoming the weaknesses of the pure CM in narrowband systems and preserving some of its advantages (e.g., immunity to Doppler shift) was proposed by Wysocki (8). The method referred to as generalized chirp modulation (GCM) is based on setting a relationship between a modulating signal $m(t)$ and an instantaneous value $\phi(t)$ of the information-carrying phase component by means of the different equation

$$\frac{d^2}{dt^2}[\phi(t)] = 2\pi h m(t) \tag{10}$$

Therefore, $\phi(t)$ is expressed as

$$\phi(t) = 2\pi h \int_0^t \int_0^\tau m(\vartheta)\, d\vartheta\, d\tau \tag{11}$$

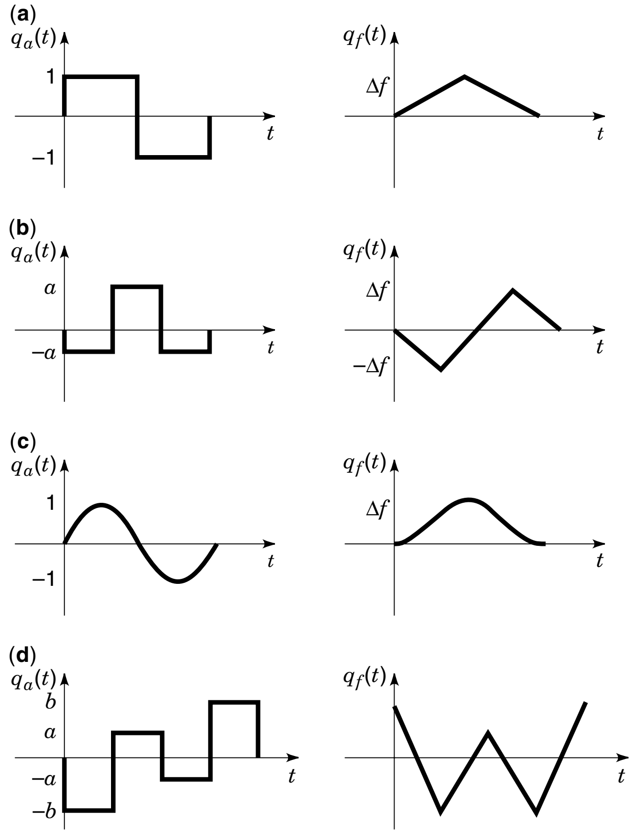


**Figure 2.** Examples of balanced modulating pulses $q_a(t)$ and the corresponding elementary frequency pulses $q_f(t)$: (a) Double chirp, (b) triple chirp, (c) sinusoidal chirp, (d) quadruple chirp.

and for the isochronous sequence $\boldsymbol{I}$ of modulating data, Eq. (11) takes the form

$$\phi(t, \boldsymbol{I}) = 2\pi h \sum_{k=0}^{N} I_{\mathrm{k}} \int_0^t \int_0^\tau q_{\mathrm{a}}(\vartheta - kT)\, d\vartheta\, d\tau \tag{12}$$

where $q_{\mathrm{a}}(t)$ is an elementary modulating pulse and $N$ is the number of a current data symbol. To achieve a possible physical realization (i.e., a limited value of an instantaneous frequency of the modulated signal), it is necessary to ensure the nonexistence of a constant component in the modulating signal $m(t)$. This can be done either by the use of balanced modulating pulses—that is, pulses fulfilling the condition

$$\int_{-\infty}^{\infty} q_{\mathrm{a}}(\tau)\, d\tau = 0 \tag{13}$$

or by ensuring that a running digital sum, $\sigma(N)$, of modulating data

$$\sigma(N) = \sum_{k=0}^{N} I_{\mathrm{k}} + \sigma(0) \tag{14}$$

is bounded.

Examples of modulating pulse shapes satisfying the condition of Eq. (13) are given in Fig. 2. The modulation scheme obtained by use of polar (+1, −1) data and the pulse shape given in Fig. 2(a) have been considered by Wysocki (13), while the scheme using pulses of Fig. 2(b) has been named the triple chirp modulation and investigated by Wysocki and Weber (14). Interestingly, the scheme utilizing pulses of Figure 2(c) is equivalent to continuous phase frequency shift keying (CPFSK) with raised cosine modulating pulses (5).

It is simple to prove that neither unipolar nor bipolar binary uncorrelated data can satisfy the condition of Eq. (14) (5). This can be achieved only by a premodulation encoding, when a balanced line code is employed. The class of balanced line codes is a very broad one (5) (e.g., AMI, PST, 4B3T, HDB3). Certainly, the modulated signal obtained as a result of different premodulation encoding has a different performance. To choose the most suitable line code, let us consider an instantaneous value of the modulated signal frequency deviation $\Delta f(t)$ given by

$$\Delta f(t) = \frac{1}{2\pi}\left[\frac{d}{dt}\,\phi(t,\boldsymbol{I})\right] = h\sum_{k=0}^{n} I_{\mathrm{k}}\int_{0}^{t} q_{\mathrm{a}}(\tau - kT)\,d\tau$$
$$= h\sum_{k=0}^{N} I_{\mathrm{k}} q_{\mathrm{f}}(t - kT) \tag{15}$$

where $q_{\mathrm{f}}(t)$ is an elementary frequency pulse.

From Eq. (15) we can notice that, apart from the scaling function of the modulation index $h$, the maximum frequency deviation $\Delta f_{\mathrm{m}}$ depends on the shape of the elementary frequency pulse $q_{\mathrm{f}}(t)$ and on the bounds of $\sigma(N)$. For example, assumming a rectangular elementary modulating pulse $q_{\mathrm{a}}(t)$ leading to a full response signaling (FRS) (5)

$$q_{\mathrm{a}}(t) = \begin{cases} \dfrac{1}{T^2}, & 0 < t \le T \\ 0, & \text{otherwise} \end{cases} \tag{16}$$

the elementary frequency pulse $q_{\mathrm{f}}(t)$ is given by

$$q_{\mathrm{f}}(t) = \begin{cases} 0, & t \le 0 \\ \dfrac{t}{T^2}, & 0 < t \le T \\ \dfrac{1}{T}, & T < t \end{cases}$$

and the instantaneous value of the frequency deviation $\Delta f(t)$ is expressed as

$$\Delta f(t) = \frac{h}{T}\sum_{k=0}^{N-1} I_{\mathrm{k}} + hI_{\mathrm{N}}\frac{t-(N-1)T}{T^2}$$

Substituting $\sigma(N)$ defined by Eq. (14) for the sum yields

$$\Delta f(t) = \frac{h}{T}\,\sigma(N-1) + hI_{\mathrm{N}}\frac{t-(N-1)T}{T^2}$$

Thus, in the considered case, $\Delta f_{\mathrm{m}}$ is proportional to the maximum deviation of $\sigma(N)$ for the applied premodulation code. In the general case, the relation between the deviation of $\sigma(N)$ of the premodulation code and $\Delta f_{\mathrm{m}}$ is not as simple as for the modulating pulse described by Eq. (16). However, with regard to the bandwidth utilization, variations of $\sigma(N)$ for the premodulation code should be as low as possible. Therefore, the optimal line code for premodulation encoding for GCM is alternate mark inversion (AMI) code, characterized by minimal variations of $\sigma(N)$ being equal to 1.

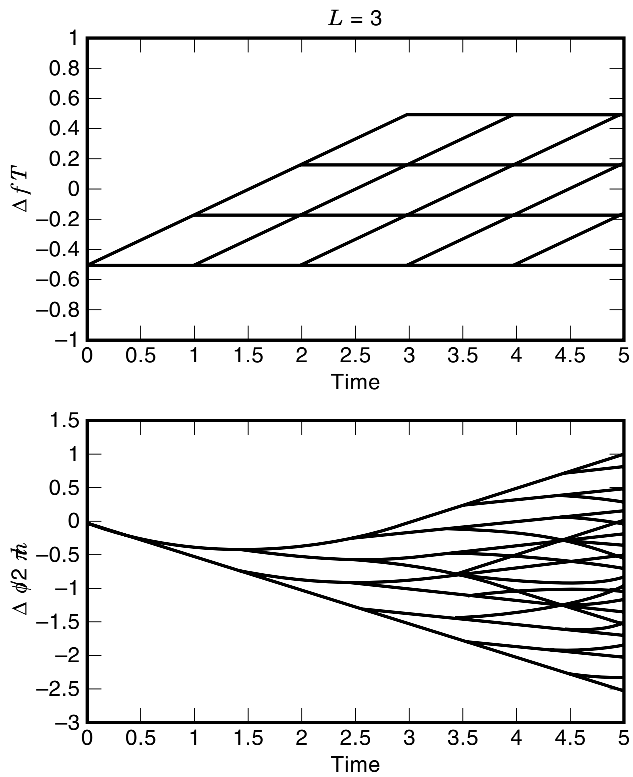


**Figure 3.** Bounded instantaneous frequency and smooth phase trajectories for PRS GCM, $L = 3$.

Examples of instantaneous frequency and phase trajectories for PRS GCM, $L = 3$, with AMI premodulation encoding (AMI-GCM) are presented in Fig. 3. It is clearly visible that the frequency deviation $\Delta f_{\mathrm{m}}$ is bounded.

A complete analysis of GCM signals AMI-GCM is presented in Ref. (8) for the case of rectangular pulses $q_{\mathrm{a}}(t)$ and for both FRS and partial response signaling (PRS) scenarios. Further information on this topic, including analysis of AMI-GCM signals with nonlinear pulses $q_{\mathrm{a}}(t)$, is available in Ref. (15). All modulation schemes considered in Refs. (8) and (15) are, for some values of modulation parameters, characterized by better spectral efficiency and better error performance in the AWGN channel than equivalent CPFSK. Thus, the AMI-GCM concept can be utilized to design robust narrowband CPM schemes.

### Hybrid Chirp Modulations

In the previous subsection, we considered the use of GCM as an alternative to CPFSK in the narrowband communication systems. Previously, we considered the use of CM in SS communications, where spreading is obtained by means of chirp pulses. The inherent capability of interference rejection makes this type of modulation a good candidate in SS systems, particularly because of a low Doppler sensitivity (16). In addition, generation and correlative reception of such pulses can be easily accomplished by the use of digital signal processing or high-performance surface acoustic wave (SAW) devices, which provide near-optimum chirp filter characteristics (17). Even better performance can be obtained if CM is combined with another form of modulation, like multilevel phase shift keying (MPSK) or additional coding. The following three subsections describe three examples of hybrid chirp modulations.

**Chirp Modulation Combined with Pseudonoise Coding.** Substantially improved antijam and antimultipath performance can be obtained if CM is combined with additional spreading by the use of pseudonoise (PN) coding. Such concepts have been considered by several authors (e.g., see Refs. 18 and 19). Use of the PN coding over CM signals allows also for creation of a multiuser code division multiple access (CDMA) system (5).

The modulated signal $c_p(t, \boldsymbol{I})$ in these systems is mathematically described by the following expression:

$$c_P(t, \boldsymbol{I}) = A \sum_{k=1}^{\infty} \xi_P(t - kT, I_k) \tag{17}$$

where

$$\xi_P(t, I_k) = \begin{cases} g(t) \cos\left[2\pi \left(f_c - \dfrac{I_k h}{2T}\right) t + \dfrac{\pi I_k h t^2}{T^2} + \phi_k\right] & 0 < t \le T \\ 0 & \text{otherwise} \end{cases} \tag{18}$$

and $g(t)$ is a spreading waveform given by

$$g(t) = \sum_{i=0}^{N-1} c_i P(t - iT_c) \tag{19}$$

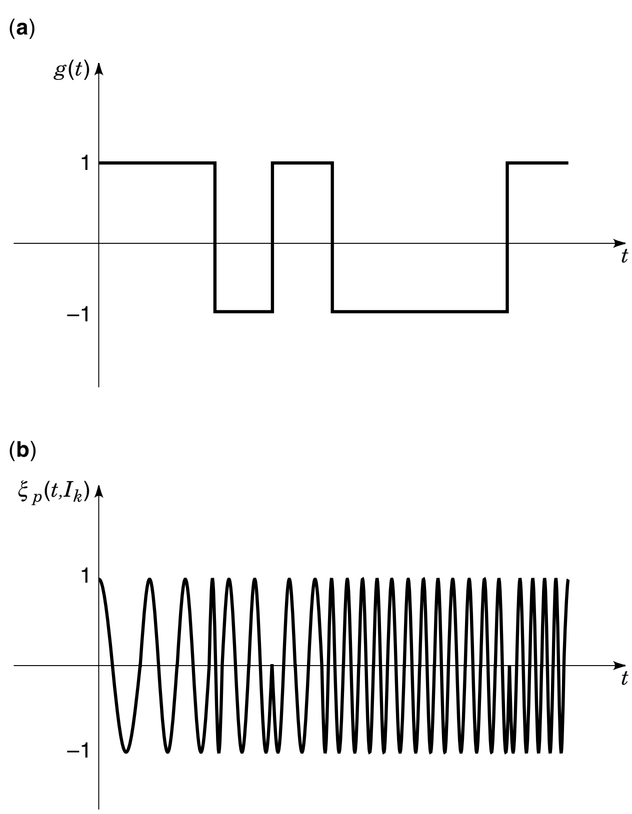


**Figure 4.** Illustration of chirp modulation combined with pseudonoise coding: (a) 8-bit spreading code, (b) positive chirp pulse spread by this code.

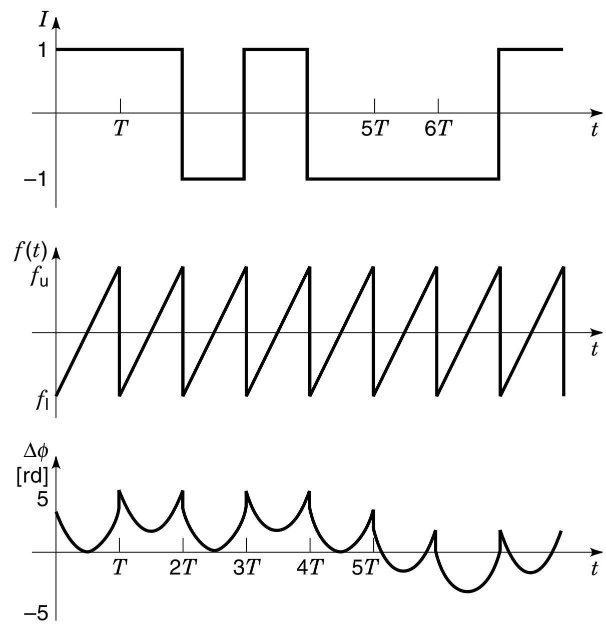


**Figure 5.** Illustration of the CM-BDPSK: (a) modulating data, (b) instantaneous frequency of the modulated signal, (c) instantaneous phase of the modulated signal with visible phase shifts due to BDPSK.

with $c_i$ being symbolic of a spreading code, $c_i = \pm 1$, and $P(t)$ being a pulse defined by

$$P(t) = \begin{cases} 1, & 0 < t \le T_c \\ 0, & \text{otherwise} \end{cases}$$

$T_c$ is the duration of single PN code symbol, usually referred to as the chip duration (5), and $N$ is the number of PN sequence symbols per single chirp pulse. Figure 4 presents an example of a positive chirp pulse combined with 8-bit spreading code.

The performance of such schemes was analyzed under different jamming conditions (19,20), and there was significant improvement in the error performance of the schemes compared with pure CM or conventional direct sequence (DS) SS systems, where, instead of CM, phase shift keying (PSK) is employed (5). This benefit, however, is partially offset by the increase in bandwidth occupied by modulated signals and therefore can be attributed to an increased processing gain of resulting SS signals (5).

### Chirp Modulation Combined with Phase Shift Keying

The concept of combining CM with PSK (CM-PSK) has been studied in Ref. 9. In the proposed scheme, the carrier wave is phase modulated by data and spread by an auxillary linear FM within each modulated signal symbol. Only one type of chirp pulse is used, either positive chirp or negative chirp. The modulation concept is illustrated in the Fig. 5, which shows how the instantaneous frequency and the phase of CM-PSK depend on the modulating data in the case of CM combined with binary differential PSK (BDPSK).

The detection of CM-PSK signals can be performed by dividing the received signal into subbands, and detected with-out using matched filters (9). The error performance of a system utilizing CM-PSK can be significantly better than that of a system utilizing equivalent plain PSK in the case of multipath environments and frequency selective jamming (9). No comparison has been made, however, between CM-PSK and DS-SS having the same spreading ratio (5).

### Direct Sequence Spread Spectrum Combined with Multiple Chirps

One of the applications being considered for DS-SS systems are high-data-rate WLANs, where the spreading is utilized not only to achieve frequency diversity (5) but also to implement multiple access to the radio channel by means of CDMA (5). The main problem, however, associated with CDMA use for WLANs stems from the fact that the bandwidth available for such systems is on the order of tens of megahertz while a data rate of several megabits per second is required. Therefore, the processing gain of the spread spectrum is very low and, consequently, in-band jammers, like other channels of the same CDMA-based WLAN, may block the communications.

The low available bandwidth and high data rate per channel require the use of short-length spreading codes that are characterized by high off-peak autocorrelation (5) and high cross-correlation between nonsynchronized codes. In an indoor environment, where multipath propagation is a serious problem and transmitters are generally located at different distances from the receiver, the aforementioned properties of short spreading codes are the source of high interference among network users and self-jamming by means of intersymbol interference (ISI).

A significant improvement in the correlation properties of transmitted signals can be achieved if the DS-SS scheme is combined with multiple chirp modulation (21). Unlike with CM-PSK, we would like here to introduce, due to the carrier modification, as low additional spreading as possible because of the spreading introduced already by applied spreading codes. Study of several possible modifications revealed that the best improvement in correlational properties of the DS CDMA signal can be obtained with a minimal increase in the occupied bandwidth, if double or quadruple chirp pulses [see Figs. 2(b) and 2(d)] are applied.

Hence, the corresponding to $i$th channel modulated signal $s_i(t)$ is described as

$$s_i(t) = Ag_i(t)\cos\left[2\pi f_c t + 2\pi\int_0^t w(t)\,d\tau + \phi(t,\boldsymbol{I}) + \phi_0\right] \quad (20)$$

where $\phi(t, \boldsymbol{I})$ is the information-carrying phase component, usually obtained by means of BPSK or QPSK (5), and the modified carrier wave $\chi_M(t)$ is given by

$$\chi_M(t) = A\cos\left[2\pi f_c t + 2\pi\int_0^t w(t)\,d\tau + \phi_0\right] \quad (21)$$

with the function $w(t)$ being either a triangular function [see Fig. 2(a)] leading to a double chirp (21) or a superposition of two triangular functions having different periods [see Fig. 2(d)] leading to a quadruple chirp (22). To obtain the desired characteristics of the modulated signal, we can optimize parameters of the function $w(t)$ for different sets of spreading codes.

**Table 1. Set of 13 Spreading Codes**

| Bipolar Sequence |
|---|
| 1 1 1 1 −1 −1 −1 −1 1 1 1 1 −1 −1 −1 −1 |
| 1 1 −1 −1 −1 −1 1 1 1 1 −1 −1 −1 −1 1 1 |
| −1 −1 1 1 1 1 −1 −1 1 1 −1 −1 −1 −1 1 1 |
| −1 −1 1 1 −1 −1 1 1 1 1 −1 −1 1 1 −1 −1 |
| 1 1 −1 −1 1 1 −1 −1 1 1 −1 −1 1 1 −1 −1 |
| 1 −1 −1 1 1 −1 −1 1 1 −1 −1 1 1 −1 −1 1 |
| −1 1 1 −1 −1 1 1 −1 1 −1 −1 1 1 −1 −1 1 |
| −1 1 1 −1 1 −1 −1 1 1 −1 −1 1 −1 1 1 −1 |
| 1 −1 −1 1 −1 1 1 −1 1 −1 −1 1 −1 1 1 −1 |
| 1 −1 1 −1 −1 1 −1 1 1 −1 1 −1 −1 1 −1 1 |
| −1 1 −1 1 1 −1 1 −1 1 −1 1 −1 −1 1 −1 1 |
| −1 1 −1 1 −1 1 −1 1 1 −1 1 −1 1 −1 1 −1 |
| 1 −1 1 −1 1 −1 1 −1 1 −1 1 −1 1 −1 1 −1 |

As an example, let us consider a DS CDMA scheme where BPSK is used as data modulation. A set of 13 (out of a possible 16) 16-bit Walsh-Rademacher functions listed in Table 1 is used as spreading codes to obtain 13 different channels operating simultaneously in the same frequency bandwidth. The function $w(t)$ has the shape shown in Fig. 2(d). Because the maximum delay that can occur between two different paths in the system is equivalent to about 50 chips, we would like the period $T_M$ of the function $w(t)$ to be greater than 50 chips (say, 64 chips, which is equal to the duration time of four data bits).

Therefore, $w(t)$ can be expressed as

$$w(t) = \sum_{k=0}^{\infty}\alpha_1\left[Tr\left(\frac{t-kT}{16T_c}\right) + \alpha_2 Tr\left(\frac{t-kT}{32T_c}\right)\right]$$

where

$$Tr(t) = \begin{cases} -2(t-0.5), & 0 \le t < 1 \\ 2(t-1.5), & 1 \le t < 2 \\ 0, & \text{otherwise} \end{cases}$$

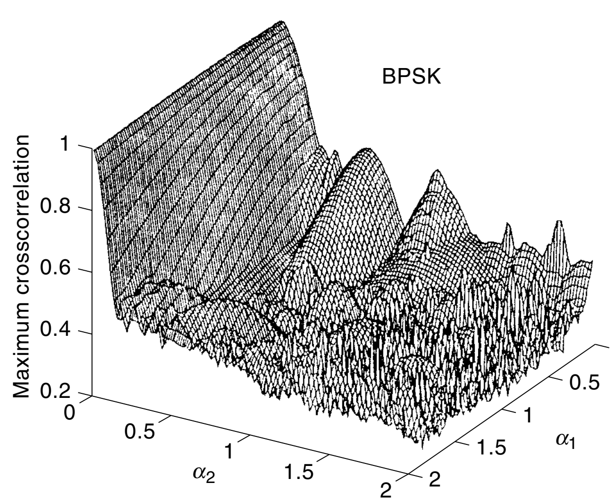


**Figure 6.** Plot of maximum crosscorrelation magnitude between any two possible channels as a function of the parameters $\alpha_1$ and $\alpha_2$ for the described example system. For some values of $\alpha_1$ and $\alpha_2$, reduction is very significant.

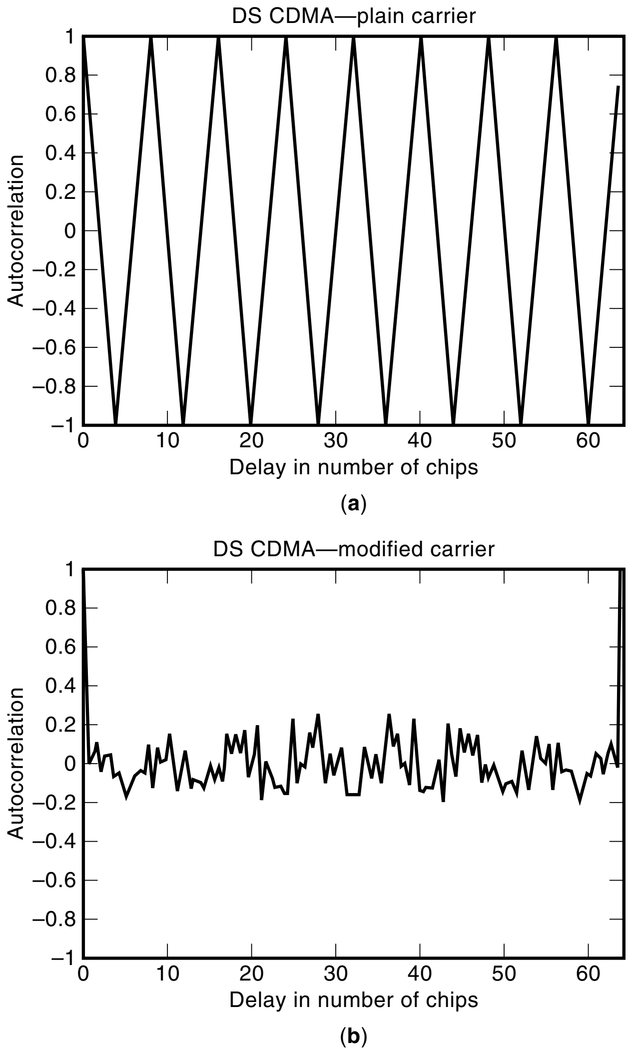


**Figure 7.** Improvement in the signal autocorrelation for the spreading sequence 1,1,1,1,−1,−1,−1,−1,1,1,1,1,−1,−1,−1,−1,1,1,1,1: (a) plain carrier wave, (b) modified carrier.

The parameters $\alpha_1$ and $\alpha_2$ can be optimized to achieve the minimum crosscorrelation between any possible pair of signals corresponding to different channels. The plot of maximum crosscorrelation magnitude between any pair of the system channels irrespective of the relative delay versus the parameters $\alpha_1$ and $\alpha_2$ is given in Fig. 6. It is clearly visible that for some values of $\alpha_1$ and $\alpha_2$ the crosscorrelation between different signals is greatly reduced, compared with the plain DS CDMA that corresponds to $\alpha_1 = \alpha_2 = 0$.

The described system is also characterized by much better autocorrelational properties. An example plot of a single-channel autocorrelation versus delay is given in Fig. 7, with the plot of Fig. 7(a) obtained for the plain DS CDMA and the plot of Fig. 7(b) obtained for DS CDMA with the modified carrier. The improvement in the autocorrelational properties translates into a lower susceptibility to ISI caused by the multipath propagation, and also facilitates synchronization of the system.

Because of the relatively low values of $\alpha_1$ and $\alpha_2$, the additional spreading due to the modification of the carrier wave is insignificant compared with the spreading introduced by the DS algorithm (5).

## SPECTRAL ANALYSIS

One of the most important characteristics of any modulated signal is its power spectral density (PSD), sometimes referred to simply as power spectrum. Knowing the PSD of the signal, we can estimate the bandwidth occupied by the signal itself or, in other words, the frequency band required for its transmission. There are several methods to calculate the PSD of digitally modulated signals (5,23); however, closed formulas can be derived for some classes of simple modulations only. For other more complicated modulations (e.g., the hybrid CM class as described in the previous section), the easiest method to estimate PSD is by computer simulation methods (e.g., Welch's estimation of PSD) (24). In the following two subsections we will show the results of PSD analysis for the pure CM and estimation results for AMI-GCM. The spectral characteristics of hybrid CMs depend strongly on the type of additional signal processing performed on the modulated signal, and therefore it is difficult to reach any general conclusion related to the PSD of such schemes. Generally, however, we can say that application of CM, apart from any other signal processing or modulation techniques employed, causes spreading and flattening of PSD characteristics.

### Power Spectra of Pure Chirp Modulation

The pure CM signal is described by Eqs. (8) and (9) in the time domain as a function of both time and data. Therefore, to find its PSD, we need to make an assumption about the statistics of modulating data. For simplicity of analysis, let us assume hereafter that for the pure CM we deal with uncorrelated binary data $I_k$, $k = 0, \pm 1, \pm 2, \ldots$, which can take the values of $+1$ and $-1$ with the probabilities

$$P\{I_k = 1\} = p, \quad p\{I_k = -1\} = q, \quad p + q = 1$$

There are two possible baseband pulse shapes $b(t, -1)$, and $b(t, 1)$, which, because of nonoverlapping [see Eq. (7)], are uncorrelated as well and appear in the random sequence $\beta(t, \boldsymbol{I})$, given by Eq. (9), with the probabilities

$$\begin{aligned} &P\{b(t-kT, I_k) = b(t-kT, -1)\} = q, \\ &P\{b(t-kT, I_k) = b(t-kT, 1)\} = p, \quad k = 0, \pm 1, \pm 2, \ldots \end{aligned} \tag{22}$$

If the carrier frequency $f_c$ is much higher than the bandwidth occupied by the CM signal, as is often the case, we can fully characterize the PSD of the CM signal by the PSD of the baseband sequence $\beta(t, \boldsymbol{I})$.

To calculate the PSD of $\beta(t, \boldsymbol{I})$, it is convenient to utilize the method described in Ref. (23) with the modification introduced in Ref. 25. As is generally the case of CPM signals with equivalent baseband pulses introducing the phase increment $\Delta\phi = 0$, the PSD of CM consists of both discrete $S_d(\omega)$ and continuous $S_c(\omega)$ components of the power spectrum (26).

The discrete component $S_d(\omega)$ is given by (25)

$$S_d(\omega) = \frac{2\pi}{T^2} |\overline{B}(\omega)|^2 \sum_{n=-\infty}^{\infty} \delta\left(\omega - \frac{2\pi n}{T}\right) \tag{23}$$

where $\overline{B}(\omega)$ is the Fourier transform of an average pulse $\overline{b}(t)$

$$\begin{aligned}\overline{B}(\omega) &= \mathscr{F}\{\overline{b}(t)\} = \mathscr{F}\{pb(t,1) + qb(t,-1)\} \\ &= p\mathscr{F}\{b(t,1)\} + q\mathscr{F}\{b(t,-1)\} = pB_1(\omega) + qB_2(\omega)\end{aligned}$$

and $\delta(\cdot)$ is Dirac's delta function (23).

The continuous component of PSD, $S_c(\omega)$, is expressed (24,25) as

$$S_c(\omega) = \frac{1}{T}\left[2\,\mathrm{Re}\sum_{k-1}^{2}\sum_{m=1}^{2} H_k(\omega)\tilde{H}_m(\omega)p_k Q_{k,m} - \sum_{k=1}^{2} p_k|H_k(\omega)|^2\right] \tag{24}$$

where

$$\begin{aligned}H_1(\omega) &= \mathscr{F}\{b(t,1) - \overline{b}(t)\} = B_1(\omega) - \overline{B}(\omega)\\ H_2(\omega) &= \mathscr{F}\{b(t,-1) - \overline{b}(t)\} = B_2(\omega) - \overline{B}(\omega)\end{aligned}$$

and $\tilde{H}_m(\omega)$ denotes the complex conjugate value of $H_m(\omega)$,

$$p_1 = p, \quad p_2 = q$$

$Q_{k,m}$ is an element of a matrix $Q$ given by Ref. 25,

$$Q = \begin{bmatrix} 1-pz & -qz \\ -pz & 1-qz \end{bmatrix}^{-1} = \frac{1}{1-pz-qz}\begin{bmatrix} 1-qz & qz \\ pz & 1-pz \end{bmatrix}$$

and the coefficient $z$ is equal to $z = \exp(j\omega T)$.

The Fourier transforms of CM pulses can be derived using formulas given in Ref. 27. They are as follows:

$$B_1(\omega) = \frac{AT}{2}\sqrt{\frac{1}{2h}}(1 + je^{-j0.5\pi})(e^{j\eta^2} - e^{-j\xi^2})\{[C(\xi) - C(\eta)] - j[S(\xi) - S(\eta)]\} \tag{25}$$

$$B_2(\omega) = \frac{AT}{2}\sqrt{\frac{1}{2h}}(1 + je^{-j0.5\pi})(e^{-j\xi^2} - e^{j\eta^2})\{[C(\xi) - C(\eta)] + j[S(\xi) - S(\eta)]\} \tag{26}$$

where the coefficients $\eta$ and $\xi$ are given by

$$\eta = \frac{\omega - \pi h}{2\sqrt{\pi h}}, \xi = \frac{\omega + \pi h}{2\sqrt{\pi h}}$$

and $C(x)$ and $S(x)$ are Fresnel's functions (28):

$$\begin{aligned}C(x) &= \sqrt{\frac{1}{2\pi}}\int_0^x \cos(t^2)\,dt\\ S(x) &= \sqrt{\frac{1}{2\pi}}\int_0^x \sin(t^2)\,dt\end{aligned}$$

The example plot of a continuous component of PSD for a CM signal with the modulation index $h = 77\pi$ is given in Fig. 8.

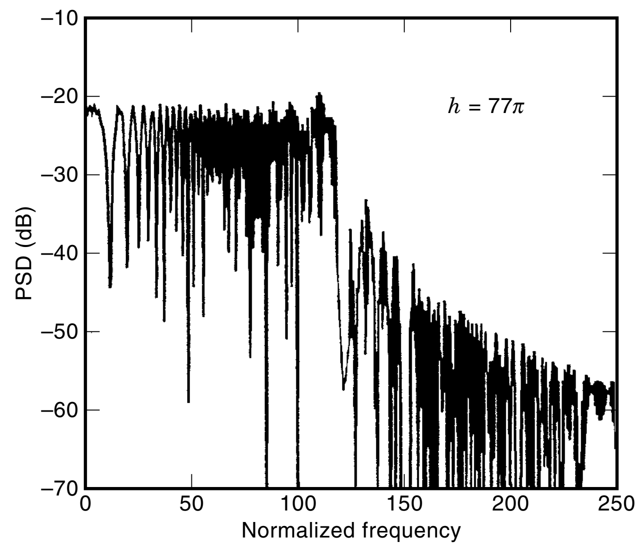


**Figure 8.** Bandwidth occupied by the broadband CM ($h \gg 1$) is approximately equal to $h$.

As we could expect, the plot is almost flat within the bandwidth required for transmission, therefore ensuring good spreading of signal power.

### Power Spectra for AMI-GCM

For any modulation, the PSD strongly depends on the shape of the elementary modulating pulse, and AMI-GCM is not an exception to this rule. In the case of "smooth" modulating pulses, like a raised cosine pulse or gaussian pulse, as well as in the case of rectangular pulses (5), AMI-GCM outperforms CPFSK in terms of bandwidth occupancy for the same values of modulation index and other pulse shapes while preserving almost the same immunity to white noise (15). As an example, in Table 2 we have compared the normalized bandwidths $B_{99}$ containing 99% of signal power for FRS AMI-GCM and FRS CPFSK with rectangular pulses (15). The spectral properties of AMI-GCM, which are better than equivalent CPFSK, are also visible in Fig. 9, where the plots of PSD for FRS AMI-GCM and equivalent FRS CPFSK are shown for some values of modulation index $h$. It is worthwhile to note that because AMI-GCM is proposed as a narrowband scheme, the values of $h$ are lower than 1.

## CURRENT AND FUTURE APPLICATIONS

Chirp modulation and related modulation schemes, although possessing characteristics suitable for mobile systems and

**Table 2. $B_{99}$ for FRS AMI-GCM and FRS-CPFSK with Rectangular Modulating Pulses**

| | FRS-CPFSK | | | FRS AMI-GCM | | |
|---|---|---|---|---|---|---|
| $h$ | $L = 1$ | $L = 2$ | $L = 3$ | $L = 1$ | $L = 2$ | $L = 3$ |
| 0.5 | 1.22 | 0.92 | 0.80 | 1.04 | 0.86 | 0.76 |
| 0.4 | 1.14 | 0.80 | 0.68 | 0.95 | 0.74 | 0.65 |
| 0.333 | 1.05 | 0.71 | 0.59 | 0.87 | 0.67 | 0.58 |
| 0.25 | 0.90 | 0.60 | 0.50 | 0.75 | 0.57 | 0.48 |

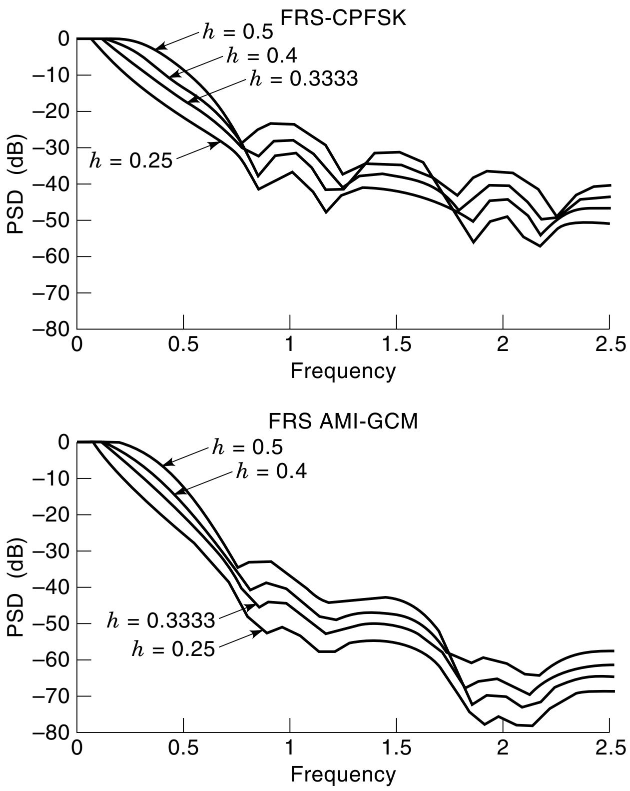


**Figure 9.** Comparison of PSD plots for FRS-CPFSK and FRS AMI-GCM.

systems working in hostile multipath and jammed environments, have never been widely employed in commercial applications. The only exceptions to date are the Consumer Electronics Bus standard of Electronics Industries Association IS-60 for data transmission through ac power wiring (10), the mainly military high-frequency radio modems (7), and currently developed applications for acoustic underwater data transmission (11). The current trends show, however, that in the future, CM together with other modulation schemes or signal processing techniques can be utilized to create robust hybrid schemes that can be successfully used in high-data-rate WLANs (9), (21).

## BIBLIOGRAPHY

1. S. L. Johnston, Radar ECCM history, *Proc. NAECON,* May 1980, pp. 1210–1214.
2. R. A. Scholtz, The origins of spread-spectrum communications, *IEEE Trans. Commun.,* **COM-30**: 822–854, 1982.
3. C. E. Cook and M. Bernfeld, *Radar Signals: An Introduction to Theory and Application,* New York: Academic Press, 1967.
4. M. R. Winkler, Chirp signals for communications. *IEEE WESCON Conv. Rec.,* 1962.
5. J. G. Proakis, *Digital Communications,* 3rd ed., New York: McGraw-Hill, 1995.
6. G. W. Barnes, D. Hirst, and D. J. James, Chirp modulation system in aeronautical satellites, *AGARD Conf. Proc. 87 Avionics Spacecraft,* NATO, Royal Aircraft Establishment: Rome, Italy, 1971, pp. 30.1–30.10.
7. L. Zhang et al., A turbo-coded, low-rate HF radio modem, in T. Wysocki, H. Razavi, and B. Honary (eds.), *Digital Signal Processing for Communication Systems,* Boston: Kluwer Academic Pub., 1997.
8. T. Wysocki, Generalized chirp modulation technique, *Eur. Trans. Telecomm.,* **6**: 679–683, 1995.
9. H. Takai, Y. Urabe, and H. Yamasaki, Anti-multipath and anti-jamming modulation/demodulation scheme SR-chirp PSK for high-speed data transmission in dispersive fading channel with interference, *Proc. VTC'94,* **2**: 1994, pp. 1355–1359.
10. D. Radford, Spread-spectrum data leap through ac power wiring, *IEEE Spectrum,* **11**: 48–53, 1996.
11. L. R. LeBlanc and P.-P. Beaujean, Multi-frequency shift key and differential phase shift key for acoustic modem. *Proc. Symp. Autonomous Underwater Veh. Technol.,* New York: IEEE, 1996, pp. 160–166.
12. T. Wysocki, Jr., *Digital Angular Acceleration Modulations* in Polish, Bydgoszcz: Academy Technology and Agriculture, 1990.
13. T. Wysocki, Jr., Error robust double chirp, *Proc. Int. Symp. Inf. Theory Appl. ISITA'94,* University of Sydney, Australia: 1994, pp. 1145–1148.
14. T. Wysocki and R. Weber, Triple chirp narrow band modulation, *Proc. 7th Eur. Conf. 'Mobile Personal Commun.,'* Brighton: IEE, Dec. 13–15 1993, pp. 90–94.
15. T. Wysocki and B. Wysocki, Narrow-band chirps, *Tech. Rep. RSL-TR 002,* Perth, Western Australia: Australian Telecommunications Research Institute, 1995.
16. R. C. Dixon, *Spread Spectrum Systems,* New York: Wiley, 1976.
17. *Surface Wave Filters: Design, Construction and Use,* H. Matthews (ed.), New York: Wiley, 1977.
18. W. I. Dolgow, S. P. Bielow, and I. D. Gorbienko, Spectral analysis of linear FM signals with inner pulse phase modulation. *Radiotechnics,* USSR, **36** (10): 66–69, 1981.
19. M. Kowatsch and J. T. Lafferl, A spread-spectrum concept combining chirp modulation and pseudonoise coding. *IEEE Trans. Commun.,* **COM-31**: 1133–1142, 1983.
20. A. K. Elhakeem and A. Targi, Performance of hybrid chirp/DS signals under Doppler and pulsed jamming, *Proc. GLOBECOM'89,* **3**: 1989, pp. 1618–1623.
21. B. J. Wysocki and T. A. Wysocki, A method to partially suppress ISI and MAI for DS SS CDMA wireless networks, *Proc. ICC'97,* 1997, pp. 899–903.
22. B. J. Wysocki and T. A. Wysocki, *DS-CDMA System for Wireless Digital Communication Channels,* Australian Provisional Pat.: Po.0302, 1996.
23. L. W. Couch II, *Digital and Analog Communication Systems,* 4th ed., New York: Macmillan, 1993.
24. P. D. Welch, The use of fast Fourier transform for the estimation of power spectra: A method based on time averaging over short, modified periodograms, *IEEE Trans. Audio Electroacoust.,* **AU-15**: 70–73, 1967.
25. T. Wysocki and M. Rydel, A method of evaluating power spectral density of digitally modulated signals (in Polish), *Proc. Polish Academy Sci., Rozprawy Elektrotechniczne,* **33**: 401–421, 1987.
26. J. B. Anderson, T. Aulin, and C.-E. Sundberg, *Digital Phase Modulation,* New York: Plenum, 1986.
27. C. E. Cook, Pulse compression—key to more efficient radar transmission. *Proc. IRE,* **48**: 310–316, 1960.
28. E. Jahnke and F. Emde, *Funktionentafeln,* Leipzig: B. G. Teubner, 1983.

TADEUSZ A. WYSOCKI
Curtin University of Technology

**CHOPPERS.** See DC-DC POWER CONVERTERS.
**CIRCLE CRITERION.** See ABSOLUTE STABILITY.
**CIRCUITAL MODEL.** See LINEAR NETWORK ELEMENTS.
**CIRCUIT ANALYSIS.** See TRANSIENT ANALYSIS.